ROYAL SOCIETY OF CHEMISTRY

PAPER

Hemp cellulose nanocrystals for functional chitosan/polyvinyl alcohol-based films for food packaging applications

Kenza Bahsaine,[ab] Brahim El Allaoui,[ab] Hanane Benzeid,[b] Mounir El Achaby,[c] Nadia Zari,[ad] Abou el Kacem Qaiss[ad] and Rachid Bouhfid [iD] *[ad]

Hemp is known for its swift growth and remarkable sustainability, requiring significantly less water, an adaptable cultivation to a wide range of climates when compared to other fibers sources, making it a practical and environmentally friendly choice for packaging materials. The current research seeks to extract cellulose nanocrystals (CNCs) from hemp fibers using alkali treatment followed by acid hydrolysis and assess their reinforcing capacity in polyvinyl alcohol (PVA) and chitosan (CS) films. AFM analysis confirmed the existence of elongated, uniquely nanosized CNC fibers. The length of the isolated CNCs was approximately 277.76 ± 61 nm, diameter was 6.38 ± 1.27 nm and its aspect ratio was 44.69 ± 11.08. The FTIR and SEM analysis indicated the successful removal of non-cellulosic compounds. Furthermore, the study explored the impact of adding CNCs at varying weight percentages (0, 0.5, 1, 2.5, and 5 wt%) as a strengthening agent on the chemical composition, structure, tensile characteristics, transparency, and water solubility of the bionanocomposite films. Adding CNCs to the CS/PVA film, up to 5 wt%, resulted in an improvement in both the Young's modulus and tensile strength of the bionanocomposite film, which are measured at (412.46 ± 10.49 MPa) and (18.60 ± 3.42 MPa), respectively, in contrast to the control films with values of (202.32 ± 22.50 MPa) and (13.72 ± 2.61 MPa), respectively. The scanning electron microscopy (SEM) images reveal the creation of a CS/PVA/CNC film that appears smooth, with no signs of clumping or clustering. The blending and introduction of CNCs have yielded transparent and biodegradable CS/PVA films. This incorporation has led to a reduction in the gas transmission rate (from 7.013 to 4.159 cm^3 (m^2 day·0.1 MPa))$^{-1}$, a decrease in transparency (from 90.23% to 82.47%), and a lowered water solubility (from 48% to 33%). This study is the inaugural effort to propose the utilization of hemp-derived CNC as a strengthening component in the development of mechanically robust and transparent CS/PVA-CNC bio-nanocomposite films, holding substantial potential for application in the field of food packaging.

Introduction

The increasing concerns about environmental pollution and food safety problems arising from the extensive utilization of petroleum-derived polymers in food packaging have driven scientists to explore eco-friendly and secure alternatives.[1] Food packaging serves a crucial function by safeguarding food from environmental risks and ensuring its freshness and safety throughout the storage and transportation processes. Additionally, it imparts valuable data to both retailers and consumers, including details on chemical content, expiration dates, storage instructions, and information about the food's origin. Moreover, food packaging plays a pivotal role in enhancing product sales with appealing colors and designs. The most sought-after characteristics in food packaging films include packaging materials that exhibit strong mechanical and thermal attributes, favourable optical qualities, biodegradability, effective barriers against water vapor, odors, and gases, along with additional functional properties like antibacterial, antioxidant, UV protection, detection, and tracking features.[2]

Petroleum-derived plastics are widely regarded as the primary materials for food packaging owing to their affordability, favourable chemical stability, exceptional barrier properties, and convenient moldability.[3] However, most of such synthetic polymers in use today lack biodegradability that results in their long-lasting presence in the environment,

[a]Moroccan Foundation for Advanced Science, Innovation and Research (MAScIR), Composites and Nanocomposites Center, Rabat Design Center, Rue Mohamed El Jazouli, Madinat El Irfane, 10100 Rabat, Morocco. E-mail: r.bouhfid@mascir.com

[b]Laboratoire de Chimie Analytique, Faculté de Médecine et de Pharmacie, Université Mohammed V de Rabat, Rabat, Morocco

[c]Materials Science and Nanoengineering Department (MSN), Mohammed VI Polytechnic University (UM6P), Lot 660 – Hay Moulay Rachid, 43150, Ben Guerir, Morocco

[d]Mohammed VI Polytechnic University, Lot 660 – Hay Moulay Rachid, 43150 Ben Guerir, Morocco

ultimately contributing to environmental contamination and posing a threat to wildlife when they are released into nature. Annually, over 500 billion plastic bags are distributed, with less than 3% of these latter being recycled, while a substantial 40% of produced plastics find their way into landfills.[4] Consequently, there has been a significant surge in research endeavours focused on developing and examining innovative environmentally friendly packaging materials. These efforts aim to mitigate the environmental consequences associated with traditional synthetic packaging materials while simultaneously ensuring product quality. In recent times, there has been notable focus on the study and manufacturing of biodegradable films derived from renewable sources.

Within this framework, the creation of packaging materials for the food industry, whether entirely or partially composed of natural and biodegradable polymers sourced from renewable materials, is proposed as a viable alternative for addressing the environmental consequences attributed to petroleum-based polymers.[5] Natural polymers emerge as the optimal substitute for traditional materials within this domain. Numerous biopolymers have been explored with the aim of creating environmentally friendly, biodegradable, and intelligent food packaging materials. Natural polymers, such as films derived from polysaccharides, proteins, and lipids, offer a range of advantageous qualities, including eco-friendliness, biodegradability, biocompatibility, edibility, and sustainability.[6] In addition to their ability to biodegrade, biopolymers possess other attributes like air permeability, sealing at lower temperatures, and cost-effectiveness when compared to synthetic polymers.

Natural fibers have undoubtedly contributed to our daily economic growth as well as our sustainability. In particular, significant interest has been accorded to natural fibers in the area of composite materials and are also considered a potential alternative to classic reinforcement items, considering their availability, biodegradability, economical, ultra-lightweight as well as eco-friendliness.[7,8] Furthermore, they have been implicated extensively in a number of industrial products namely adsorbents, packaging, materials construction, paper, as well as textiles products.[9,10] Natural fibers offer also impressive physicomechanical characteristics that lead to the emergence of special composites materials containing especially lignocellulosic fibers. Cellulose, hemicellulose, lignin, pectin, and wax are the primary components of these materials, whereas cellulose representing their major constituent.[8]

Cellulose is by a significant margin the natural polymer that can be found in the greatest abundance all over the earth. The global production and decomposition of cellulose is about 1.5 $\times 10^{12}$ tons a year compared to earth's reserves of both fossil and mineral sources.[11,12] This biopolymer accounts for approximately one-third of plant tissues that may be regenerated *via* photosynthesis.[13] Chemically speaking, cellulose biopolymer is a polysaccharide of general formula $(C_6H_{10}O_5)_n$, consisting of a linear chain composed of repeated anhydro-D-glucose moieties. Every single unit is hydrogen-bonded (intra/intermolecular bonds), resulting in ordered structural domains that are also linked with each other by amorphous structural domains leading in final to a fibrous structure.[14] There are a variety of

natural fibers from which cellulose could be obtained namely wood, bamboo, straw, bagasse, hemp, flax, kapok, cotton, and whose composition differs according to their origin, age, *etc.*,.[15] In the same context, extracting cellulose microfibers (CMf) from natural fibers is realized by alkaline and bleaching treatments, which is also used to isolate cellulose nanomaterials like cellulose nanocrystals (CNCs) as well as cellulose nanofibers (CNFs). The CNC is synthetized through hydrolysis acid process and can be exploited as reinforcement of polymeric items thanks to its outstanding features. These include mechanical properties and barrier behavior, important specific surface area of approximately 200–250 m^2 g^{-1}, great availability of hydroxyl groups, leading thus to nanomaterials development with hydrophilic surface. The surface hydrophilicity helps to disperse components with hydroxyl groups more easily in hydro-soluble polymeric matrices. Moreover, CNC is also characterized by their low-level density (estimated 1.57 g cm^{-3}), biodegradability, biocompatibility, renewability as well.[16]

Industrial raw hemp, a yearly harvested plant, is one of the underutilized sources of agricultural waste. Hemp fibers are produced from cannabis variants that are minimal in THC with no effects on the brain. The annual global production of hemp fiber is estimated at approximately 70 000 tons and almost half is manufactured in northern Europe and the other half in China.[17] The primary product grown is hemp fiber and stalks are left as waste. Indeed, the stalks are composed of cellulose, hemicellulose, lignin, and other elements in proportions of 70, 19, 5, and 4 wt%, respectively.[18] The Young's modulus of hemp is greater compared to that of any other natural fiber. One such characteristic that makes hemp fibers appropriate for use as reinforcement in composite materials is their high aspect ratio (length/width). Natural fibers are an excellent alternative to synthetic fibers such as glass, carbon, or aramid when used as reinforcing agents in composites due to their many advantageous characteristics. These include high specific strength and modulus, unrestricted and sustainable availability, low density, reduced tool wear, and improved energy recovery. Hemp fibers are becoming an increasingly attractive reinforcement option in the composites industry due to their low production cost, environmental friendliness, and biodegradability. As more and more consumers prioritize items that are good for the environment and can be recycled, this last quality has become an increasingly attractive selling point.[19] Furthermore, the increased cellulose content of hemp fiber has enticed researchers to use such natural fibers instead of conventionally obtained materials in composite manufacture.[20] For such reasons, it appears that hemp and its derived products could be one of the potential building blocks for more resilient and environmentally friendly food systems.

While remaining in the biopolymers concept, Chitosan (CS), a chitin derivative, is regarded as the second prominent polysaccharide on the entire world after cellulose. CS is composed mainly of *N*-acetylglucosamine and glucosamine units and obtained from chitin by *N*-deacetylation by alkaline treatment at high temperature. This biopolymer is distinguished by their biocompatibility, biodegradability, and non-toxicity. It can be harvested from a wide variety of marine by-products and other

renewable resources. Therefore, chitosan is a low-cost polysaccharide that is widely available in the market. The solid form of chitosan has a semi-crystalline structure and is soluble in diluted organic acids such acetic, citric, formic, lactic, malic, and tartaric.[21] Chitosan-based composites are also useful for packaging applications because of their outstanding film-forming capabilities and their ability to enhance the food's shelf life.[22,23] Furthermore, chitosan possesses antimicrobial and antioxidant characteristics as well as a bifunctional nature, regarded as one of the most essential and cost-effective biopolymers used in a variety of fields, including food preservation, medicine, and water purification.[24,25] The use of chitosan as a material for food packaging films is gaining popularity owing to the properties described above. However, compared to conventional plastics, a number of factors limit the widespread use of chitosan including high swelling in water, relatively low water vapor resistance, relatively low elongation, low toughness, and high cost.[26] In fact, polymer blending presents the most efficient approach to fabricate new materials with desirable characteristics. Additionally, it is advised to combine CS with hydrophilic materials such as poly(vinyl alcohol), poly(vinylpyrrolidone), poly(ethylene oxide), polyacrylamide, and subsequently polycaprolactone in order to achieve outstanding mechanical properties in CS-based materials.[27] The selection of PVA over other polymers is predicated on its good ability to form films, high crystallinity, non-toxicity, water-solubility, biodegradability, and ecological properties.[28] Furthermore, the utility of CNC to improve mechanical characteristics of PVA along with CS functionalized items has been highlighted by many researchers. In this respect, Perumal et al.[29] observed that the addition of CNC produced from rice straw into the PVA/CS mix polymer increased the mechanical characteristics as well as the thermal stability of the material. Similarly, the same team made bionanocomposite films using PVA and CS reinforced with CNC extracted from areca nutshell fibers. Manufactured films tensile was significantly enhanced by incorporating CNC into the PVA/CS films, moreover, the prepared films exhibited excellent antifungal and antibacterial activities.[30]

Nano-biocomposites represent a fascinating group of hybrid materials, consisting of a bio-based matrix combined with nano-sized fillers (referred to as nanofillers). This amalgamation of environmentally friendly biopolymers and nanomaterials, aimed at achieving synergistic effects, stands out as one highly innovative approach for enhancing their characteristics. Depending on the nanofiller's properties and geometry, it is possible to attain novel or enhanced attributes, such as improved gas barrier properties, increased mechanical rigidity, enhanced transparency, and heightened thermal stability. Therefore, the current investigation aimed to valorize Moroccan hemp stalk waste fibers through cellulose microfibers and cellulose nanocrystals (CMfs and CNCs) extraction, then the further dispersion of CNCs into CS/PVA blend polymer to develop CS/PVA/CNC bionanocomposite films. Moreover, the physico-chemical characteristics of both extracted CNCs and the obtained films were investigated. Still, our main focus was to examine the way the mechanical, chemical, optical and gas permeability properties of CS/PVA-based bionanocomposites items were affected using hemp stalk-derived CNCs as a reinforcing agent.

Experimental section

Materials and reagents

Raw Hemp stalks (RH) (Tangier-Tetouan-Al Hoceima region, Morocco) were pre-treated, sun-dried and ground with a 1 mm sieve using a Fritsch pulverisette 19 type grinder (Fig. 1(b)). Polyvinyl alcohol (PVA) (M_w = 61 000 g mol^{-1}), highly viscous chitosan (CS) (degree of deacetylation 85%), glycerol, sulfuric acid (H$_2$SO$_4$, 98%), sodium hydroxide (NaOH, ≥98%), sodium chlorite (NaClO$_2$, 77.5–82.5%) and acetic acid (CH$_3$COOH, >99%) all procured from Sigma Aldrich. Ultrapure water (18.2 MΩ cm, Milli-Q water) was added for PVA and CS solubilization. The received chemicals are used as they arrived and without modifications.

Extraction process of cellulose microfibers (CMfs)

The CMfs extraction has been carried out in accordance with a previously described procedure.[31] Basically, the crushed RH were washed with water for 2 h at 60 °C while maintained under continuous stirring. Following washing, the RH were given an alkaline treatment of 4 wt% sodium hydroxide then heated to 80 °C under stirring during 3 hours at reflux. After completion, the fibers were then washed several times with water by means of successive centrifugations (10 509×g and 10 °C for 10 min) until they were completely cleaned, and any remaining NaOH was removed until a neutral solution was obtained (Fig. 1(c)). Three bleaching were performed on the alkali-treated hemp fibers (AH) with an acidified solution containing sodium chlorite (1.7 wt%) at pH adjusted to 4.0–5.0 by acetic acid at temperature equal to 80 °C for 5 hours. This procedure was carried out three times in all (Fig. 1(c)).

Extraction process of CNC

BH fibers were subjected to a treatment with sulfuric acid (H$_2$SO$_4$, 64 wt%) for one hour at a temperature of 45 °C with simultaneous shaking. The hydrolyzed solution was successively washed by distilled water using SIGMA 3-18ks centrifuge at 10 509×g and 10 °C for 20 min. For 5 days, the suspension
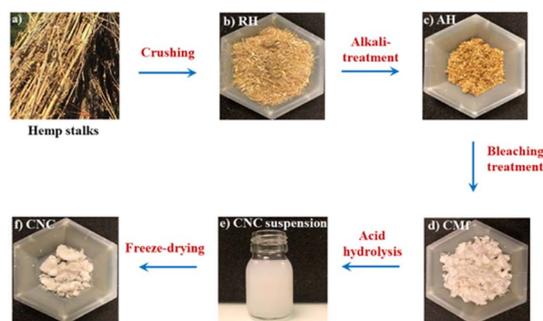
Fig. 1 General steps of CMf and CNC extraction with (a) Hemp stalks, (b) RH, (c) AH, (d) CMf, (e) CNC suspension and (f) freeze dried CNC.

was dialyzed against distilled water until a consistent pH of roughly 6–7 was attained. Before being stored in the refrigerator for later use, the obtained suspension was sonicated for 20 min (Fig. 1(e)). It is possible to acquire CNC in the form of a white powder by subjecting it to a technique known as freeze drying (Fig. 1(f)). Photographs of the RH, AH hemp, and extracted CMfs material are shown in Fig. 2.

Preparation of bionanocomposite films (CS/PVA/CNC)

A solvent casting/evaporation method was performed to develop the CS/PVA/CNC bionanocomposite films which contain 60% CS, 40% PVA, glycerol (40 mg) as well. To begin with, the dissolution of PVA (0.4 g) was performed in water preheated to 90 °C and stirred for continuous 2 h. On the other hand, 0.6 g of CS was dissociated in water acidified with 1% acetic acid and stirred for 3 h to get a homogeneous solution. Then, both solutions were blended by magnetic stirring for 1 hour right after adding an acceptable quantity of glycerol as a plasticizer. Different CNC suspensions (0–0.5–1–2.5 and 5 wt%) were obtained by adding CNC powder to ultra-pure water then were added to the CS/PVA mixture and vigorously stirred for 30 minutes. The generated blends were then placed in a Petri plate and dried for 48–72 hours at room temperature to allow the water to evaporate, leading to the elaboration of bionanocomposite films. The obtained films, namely CS/PVA/CNC-0%, CS/PVA/CNC-0.5%, CS/PVA/CNC-1%, CS/PVA/CNC-2.5%, and CS/PVA/CNC-5%, were conserved for further characterizations.

Characterization techniques

Fourier transform infrared spectroscopy (FTIR) study was undertaken to identify the characteristic groups and the spectra were recorded by means of a spectrophotometer (FT-IR, Spectrum Two, PerkinElmer) equipped with UATR accessory, in transmission modes of 4000–400 cm^{-1}.

The morphological surfaces of the cryo-fractured bionanocomposite films and cellulosic materials were examined by

scanning electron microscopy (Thermo Scientific™ Quattro ESEM), and the micrographs were taken with a Quatro S, operating at 30 kV.

An optical microscope (OM) type (Eclipse LV100ND, Nikon) was used to examine the hemp microstructure and changes occurred in its shape. Each representative sample was photographed after being positioned on a clean glass sheet. Atomic Force Microscopy (AFM) type (Veeco Dimension Icon) investigations were conducted to assess the dimension and morphology of the extracted CNC.

The transparency of the bionanocomposite films was studied using a UV-vis spectrophotometer (UV-1900 SHIMADZU) at wavelength between 200 and 800 nm by measuring their transmittance. The bionanocomposite samples were positioned directly on the side of the magnetic cell of the spectrophotometer with an empty test cell serving as a reference.

A universal testing machine (H10KT, Tinius Olsen) was used to test all rectangular specimens with a crosshead speed of 3 mm min^{-1} at ambient temperature. The tensile features were assessed regarding Young's modulus, tensile strength, and elongation at break of both CS/PVA free CNC and CS/PVA/CNC nanocomposites films to obtain a clear insight into the influence of chemical alteration as well as the integration of CNC.

Oxygen permeability was measured using a gas permeation instrument (VAC-V1 Gas Permeability Tester, LABTHINK®) in accordance with ASTM D1434. All of the available specimens were subsequently sliced as discs of 15 cm diameter and 60 μm thickness. Measurements are then maintained till the oxygen permeability level is stable.

After being submerged in water over a period of 24 h, a film's water solubility is measured by the percentage of its dry matter that has been dissolved. In an oven set to 50 °C, each sample was allowed to dry until it reached a constant weight. The films were uniformly thick and cut into a size of about 30 × 30 mm. Following that, each specimen was then placed into a beaker with 50 mL of distilled water and kept at 23 °C for 24 hours. After being removed from the water, the films were returned to the oven and kept there until they reached a weight that was consistent in order to establish the film's ultimate dry weight. The film solubility was obtained using the following eqn (1):

$$\text{Water solubility}(\%) = \left(\frac{W_i - W_f}{W_i} \right) \times 100\% \quad (1)$$

where W_i and W_f are the initial and final weight of the samples.

Results and discussion

Characterization of bleached fibers and CNC extracted from Hemp

Fourier transform infrared spectroscopy (FTIR). As can be seen in Fig. 3, Fourier transform infrared spectroscopy was used to assess the chemical constitution and surface functioning of RH, AH, CMf, and CNC materials. Both RH as well as AH samples exhibited a typical cellulose absorption peak at 3335 cm^{-1}, indicating the stretching vibration of the hydrogen-bonded hydroxyl group (–OH).[32] Moreover, two different peaks seen at 2915 cm^{-1} and 2848 cm^{-1} are related to asymmetric and

Fig. 2 Photograph of (A) RH, (B) AH, (C) BH and (D) acid hydrolyzed suspension Hemp fibers.
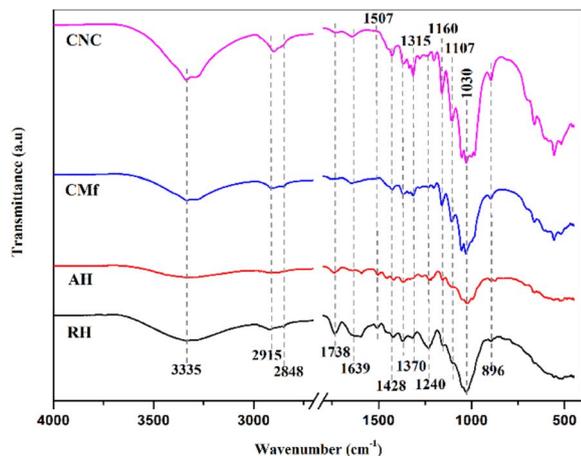
Fig. 3 Fourier transform infrared curve of RH, AH, CMf and CNC.

Fig. 4 Hemp fiber observed under optical microscope and SEM: (a) RH, (b) AH (d) CMf and (d) CMf diameter.

symmetric from (CH$_2$) moiety.[33,34] Additionally, both wavelengths at 1738 cm^{-1} and 1240 cm^{-1} refer to the C=O groups in lignin and hemicellulose,[35] whereas the low intensity of the 1507 cm^{-1} peak represents the lignin C=C groups. Their intensity in the AH spectrum is reduced, implying that hemicellulose and lignin may have been partially eliminated through the alkaline treatment.[36–38] The band at 1639 cm^{-1} might be linked to binding vibration of H$_2$O absorbed through the cellulose fiber network.[39] The absorption bands found at 1428 cm^{-1}, 1370 cm^{-1}, and 1315 cm^{-1} were ascribed to CH$_2$ symmetric bending, C–O symmetric stretching, and C–H bending of cellulose, respectively.[40] In addition, bands with frequencies of 1160 cm^{-1}, 1107 cm^{-1} and 1030 cm^{-1} are linked to asymmetric C–O–C stretching, backbone vibration of C–O and bond stretching of C–O in the cellulose.[41] The tiny 894 cm^{-1} peak might be assigned to β-glycosidic bonds occurring between monosaccharides in the structure of cellulose.[34,41]

The FTIR spectrum of CMf revealed an absence of bands at 1738 cm^{-1}, 1507 cm^{-1}, and 1240 cm^{-1} related to lignin and hemicelluloses existence, whilst cellulose bands remained, confirming that non-cellulosic components had been successfully stripped after the application of the chemical treatment. Besides, when comparing the CNC and CMf spectra, no differences were noticed. The results demonstrate that the cellulose chemical structure is still stable after sulfuric acid hydrolysis.[42] Therefore, FTIR results are consistent with the literature, confirming the existence of the main components (cellulose, hemicellulose, and lignin) as well as effective CNC extraction.

Optical microscope/scanning electron microscopy. Optical micrographs of raw then alkali-treated fibers after grinding are illustrated in Fig. 4. This latter shows distinctives changes after NaOH treatment. The photomicrographs of the untreated fibers (Fig. 4(a)) appear to be shiny, dark green colored, and composed of several strongly attached fibers covered with non-cellulosic substances comprising pectin, hemicellulose, lignin, and others.[43] This would suggest that the fibrous hemp structure is composed of cellulose microfibrils coated with hemicellulose and lignin.[44] Natural fibers that have been alkali-treated with
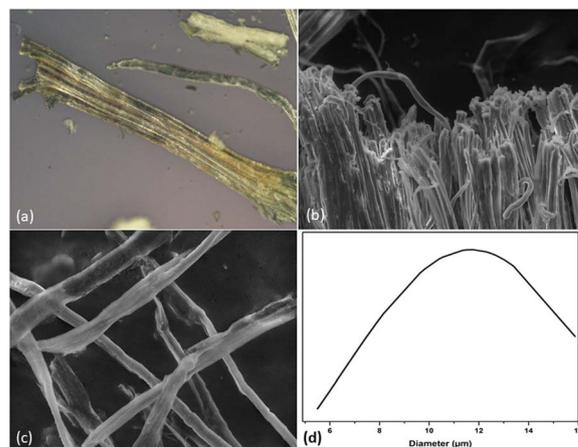
NaOH (Fig. 4(b)) results in the absence of glossy surface without destruction of this latter.[45] These changes are mainly due to partial suppression of non-cellulosic compounds, and the striations along the fiber's length become more distinct. After bleaching treatment, cellulose fibers were subjected to SEM observations, a closer look confirms the liberation of the cell walls and the release of individual cellulose fibers (Fig. 4(c)) with a diameter of 10.16 ± 2.64 μm (Fig. 4(d)).

Atomic force microscopy. Since the size of the extracted CNC is on the nanoscale, its shape, diameter, and length were identified by Atomic Force Microscopy (AFM). The observation of Fig. 5 revealed the presence of elongated and individualized nanosized CNC particles as well as some fine aggregates, indicating their successful extraction from the pre-treated hemp. Furthermore, consider using AFM images the CNC diameter was homogeneous while their length was irregular. According to the literature, it is important to underline that the exact size and morphology of CNC are essentially impacted by the feedstock nature/source along with the hydrolysis conditions or pretreatment.[46] In this context, the CNC dimensions were calculated *via* the high profile in conjunction with the CNC high sensor image
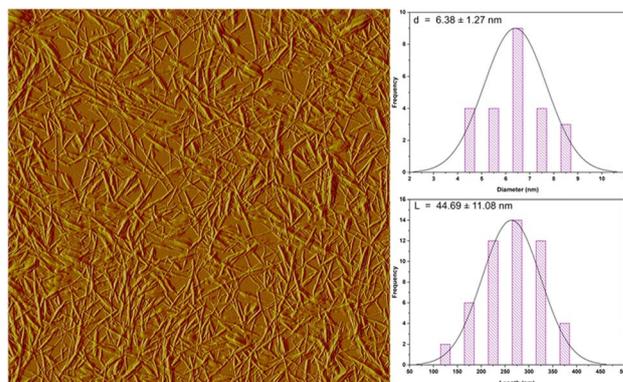
Fig. 5 AFM image of CNC.

(Fig. 5). It is obvious that the as-extracted CNC's average diameter (D) is 6.38 ± 1.27 nm, and a length (L) of about 277.76 ± 61 nm leading to an average aspect ratio around 44.69 ± 11.08.

Characterization of CS/PVA/CNC films

Fourier transform infrared (FT-IR) spectroscopy. The identification of the functional groups in the film as well as the interactions between the constituents was done using the potent instrument of FTIR spectroscopy. Fig. 6 represent the infrared spectra of CS/PVA, as well as CS/PVA/CNC films with varied CNC amount (0–0.5–1–2.5 and 5 wt%). In CS/PVA blend spectrum and in agreement with the literature, a wide band located at 3289 cm^{-1} is linked to –OH and NH$_2$ stretching vibrations of chitosan as well as hydroxyl group found in intramolecular and intermolecular hydrogen bonds of PVA (Fig. 7).[47] Both symmetric and asymmetric stretching of the chitosan CH$_2$ group could be represented by the peaks positioned at 2918 and 2883 cm^{-1}, while carbonyl bond vibration (C=O) of the amide and protonated amine group were observed at 1641 and 1558 cm^{-1}.[24] Moreover, the peak at a wavelength of about 1029 cm^{-1} is characteristic of C–O stretching vibration[48] and the band positioned at 1147 cm^{-1} is ascribed to an acetal ring development by crosslinking, which confirms the interaction between PVA and CS (hydrogen bonds Fig. 7).[49] After the insertion of CNC into CS/PVA blend, a slight shift of CNC hydroxy stretching vibration from 3337 cm^{-1} to 3282 cm^{-1} in CS/PVA/CNC bionanocomposite was observed (Fig. 6).[29] More than that, the absorption band found at 1583 cm^{-1} in pure CS spectra (N–H) is displaced to 1564 cm^{-1} in the CS/PVA/CNC FTIR curve, revealing the substantial linkages took place between NH$_3^+$ unit corresponding to CS and OSO$_3^-$ moieties of CNC (1203 cm^{-1}) (Fig. 7).

Fig. 7 Occurrence of the different interactions in CS/PVA and CS/PVA/CNC bio-nanocomposite films.

Scanning electron microscopy (SEM). Scanning electron microscopy tool provides an adequate and general view of the occurred surface phenomenon. Fig. 8 displays a series of some SEM micrographs bringing to light the surface morphology of the cryogenically fractured bare CS/PVA and loaded with CNC at different amounts (0.5–1 and 5 wt%). The analysis reveals that the neat CS/PVA film have a smooth cross-section, homogeneous, free of fissures and irregularities reflecting the strong interaction and integration of PVA into CS matrix.[50] Similarly, Fig. 8 obviously confirms that there were no visible clustering of CNC or micro-phase detachment. All shapes of CS/PVA films reinforced CNC up to 5 wt% were uniform and devoid of CNC aggregates, proving the affinity between CS/PVA mixture and CNC as well as their ability to develop homogeneous hybrid composites. The remarkable CNC distribution in the composite matrix is related to their potential in enhancing bio composites films characteristics.[51]

Film tensile properties

Survey of the literature reveals that composites reinforced natural fibers are claimed to provide mechanical characteristics like those reinforced with synthetic fibers. For this, natural

Fig. 6 Fourier transform infrared spectra of CNC, CS, CS/PVA, CS/PVA/CNC-0.5%, CS/PVA/CNC-1%, CS/PVA/CNC-2.5% and CS/PVA/CNC-5%.
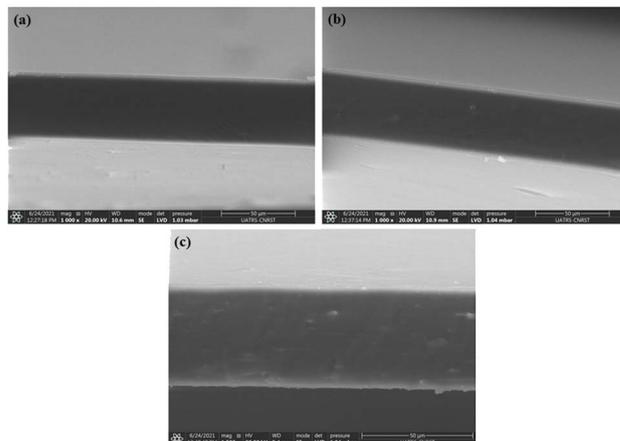
Fig. 8 SEM micrographs from the cryo-fractured surfaces of CS/PVA films reinforced with 0 wt% CNC (a), 1 wt% CNC (b), and 5 wt% (c) CNC.

fibers are able to compete with synthetic ones when evaluating strength and modulus. Tensile experiments were performed to investigate chemical modification impact on the mechanical behavior of nanocomposite films. In each sample, 3 tests were operated, and each film was cut prior into rectangular forms (length = 60 mm and a width = 10 mm). The strain–stress curves of both CS/PVA and CS/PVA/CNC films are represented in Fig. 9 from which Young's modulus (E), Tensile strength (σ_s),

Fig. 9 Stress−strain tests, young's modulus, tensile strength, and elongation at break of CS/PVA, CS/PVA/CNC-0.5, CS/PVA/CNC-2.5, and CS/PVA/CNC-5 bio-nanocomposite films.

and Elongation at break (ε_b) were calculated. The slope of the linear elastic deformation of the stress–strain curve is described as the Young's modulus, the tensile strength is defined as the highest stress value exerted on a specific sample, the strain to fracture the specimen is designated as the elongation at break. According to stress–strain patterns depicted in Fig. 9, the tensile characteristics of CS/PVA are changed by the addition of various CNC percentages (0.5–1–2.5–5 wt%). It is obvious that the CNC free CS/PVA blend film exhibited ductile behavior, low modulus of elasticity and tensile strength, which precludes its usage as a packaging material requiring then high strength and stiffness.[52] A rise in tensile modulus from 202.32 to 412.46 MPa and tensile strength from 13.72 to 18.60 MPa, a decrease in elongation at break from 71.37 to 40.88% were seen in CS/PVA/CNC films after CNC incorporation at a weight percentage up to 5%. The increase is related to the establishment of a more adhesive bond that relies on a powerful electrostatic interaction as well as hydrogen linkage occurring between CNC and the CS/PVA blend, while the elongation at break's decrease indicates that the reinforcement affects the resulting composite's ductility. The higher CNC Young's modulus appears to be responsible for the CS/PVA blend's considerable reinforcing impact on mechanical properties. Furthermore, the improved tensile characteristics of the as prepared bionanocomposite films are mainly due to the homogenous dispersion of CNC as well as desirable interfacial contacts involving CNC and the polymer matrix that result in bio-plastic films that are both mechanically robust and flexible. Such enhancements revealed that the CS/PVA/CNC bionanocomposite films exhibit a high young's modulus and strength, both of which are important mechanical qualities for food packaging applications.

Gas transmission rate (GTR)

In food preservation, the GTR (O_2) of packaging materials is critical. In order to boost good food isolation and reduce interaction with oxygen (oxidation reaction, growth of aerobic microbes), films must have strong barrier qualities. Single-component biopolymer-based films rarely met the barrier requirements of packaging materials (coffee, cheese, and fresh meat). These polymers don't have the necessary oxygen or moisture barriers, and in certain situations, they don't have either at all.[53] For such purpose, CNCs have strong mechanical strength, a high Young's modulus, a wide surface area, outstanding biodegradability, and particularly good oxygen barrier characteristics, among other qualities.[54] PVA has strong mechanical characteristics and has a high level of resistance to the infiltration of organic solvents and oils, making it an effective barrier against oxygen and odors.[55] A low GTR means that the barrier to oxygen is excellent. Therefore, an appropriate oxygen barrier in food processing systems can greatly enhance the product's quality and prolong its shelf life. Fig. 10 depicts the GTR for the manufactured CS/PVA/CNC films. As the results indicate, the GTR of CNC-modified CS/PVA films is approximately lower than the GTR of unreinforced CS/PVA films. The enhance of CNC percentage in CS/PVA bio-nanocomposites decreases the GTR value of the film. The incorporation of 0.5,
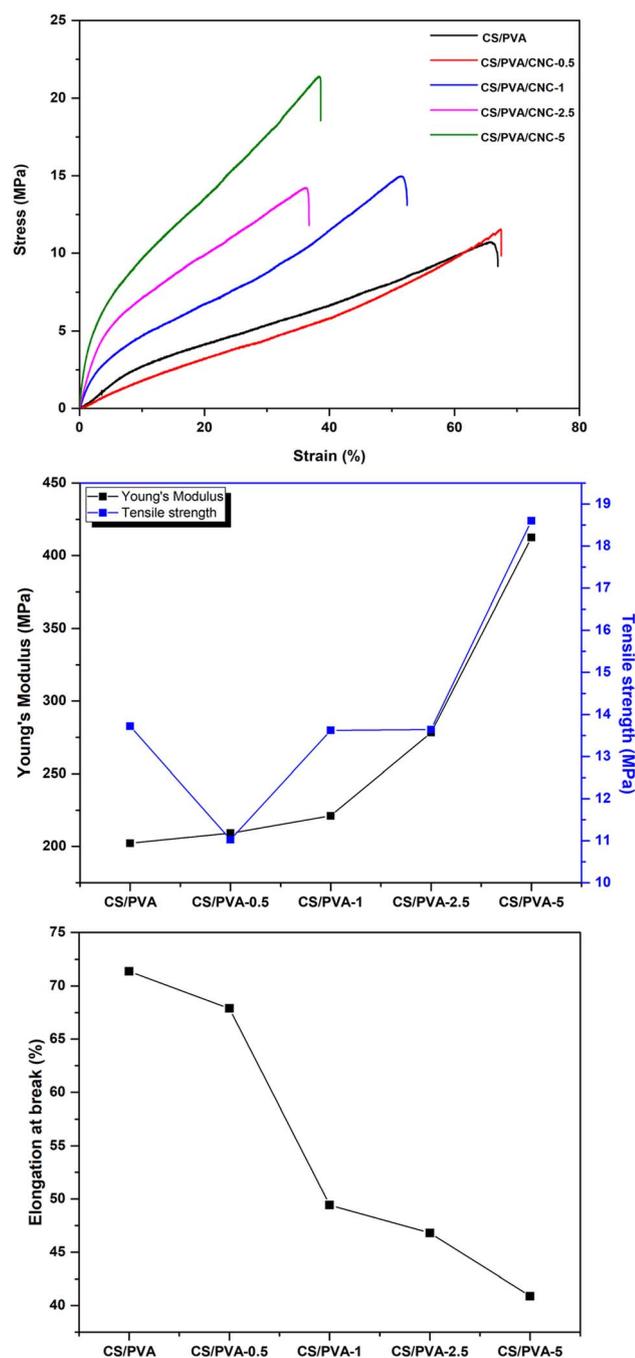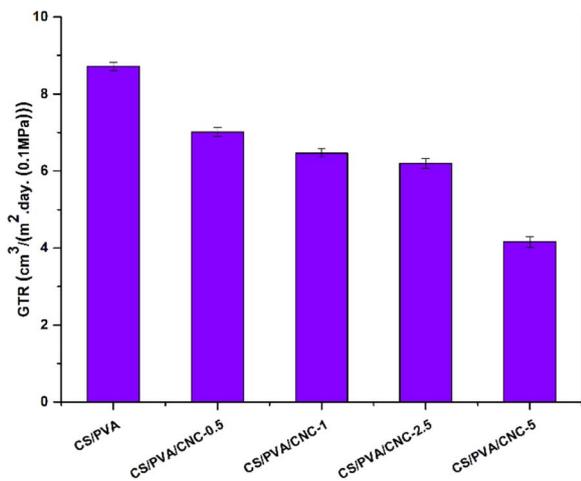
Fig. 10 The GTR of the CS/PVA films reinforced with various CNC contents (0, 0.5, 1, 2.5, and 5 wt%).

Fig. 11 UV-vis spectra of CS/PVA and reinforced CS/PVA with (0.5, 1, 2.5, 5 wt%) CNC filler.

1, 2.5 and 5 wt% of CNC considerably reduces the GTR value of the prepared films to 7.013, 6.464, 6.196, 4.159 cm^3 (m^2 day (0.1 MPa))$^{-1}$, respectively, while the unreinforced CS/PVA films achieve a GTR value of 8.715 cm^3 (m^2 day (0.1 MPa))$^{-1}$. This suggests that the incorporation of CNC might prevent oxygen molecules from moving and interacting with the units of CS and PVA. Chitosan and PVA films' vacant spots were probably filled in by CNC, which resulted in a more compact film framework. Besides, the abundance of hydroxyl groups on CNC's surface, which can build a structural network of strong hydrogen connections between chitosan and PVA, may lessen the susceptibility of film materials to oxygen molecules.[56] In response to the "tortuous idea," nanocellulose acts as a barrier that inhibits oxygen molecules from passing through films. When it comes to maintaining the freshness of fruits and vegetables by inhibiting their respiration, a biocomposite film with a lower GTR value is preferable. Given their incredibly well-oriented structure, the CS/PVA-5 biocomposite film has superior capabilities as an oxygen barrier. These results can be explained by the polymer blend's affinity for the CNC wall that fills voids attributable to its proper dispersion preventing oxygen molecules to diffuse across the film.[57]

Transparency

When it comes to using bio-nanocomposite films as a product intended for packaging, the films transparency is essential since it affects their quality. The more the film is transparent, the more it is successfully commercialized and accepted by the consumer. Fig. 11 compares the transparency of CS/PVA and CS/PVA blended polymers modified by different CNC amounts using UV visible light. The obtained results claim that the CS/PVA films have the highest degree of transparency in the region UV-visible (transmittance 90.93%) compared to modified CS/PVA films which displayed transmittance values of 90.23, 90.21, 86.17 and 82.47% for CNC concentrations of 0.5, 1, 2.5 and 5 wt%, respectively. As evident, adding CNC amounts of 0.5 and 1 wt% in the CS/PVA, both films maintained a similar
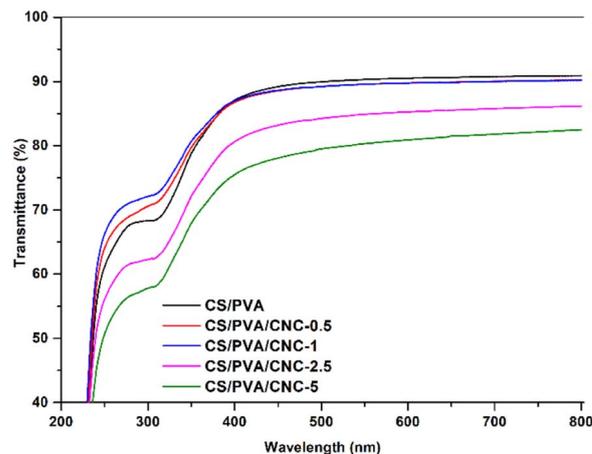
transparency to CS/PVA, which is owed to the good nanoscaled dispersion of CNC and this is further confirmed by the color which is uniformly distributed in the films.[58] While for concentrations of 2.5 and 5 wt%, the transmittance of the bionanocomposites tends to decrease slightly but remains higher than 82%. The findings indicate that the inclusion of CNC to the CS/PVA polymer blend film couldn't influence the clarity of the film. In addition, the optical images showed no agglomeration effects. As a result, the amount of light scattering is reduced, and visible light transmission across the bionano-composites is preferred. This confirms the excellent compatibility between both CNC and CS/PVA blend. Opacity serves as a well-recognized means to quantify the transparency of a film. A higher opacity value corresponds to reduced transparency.[59] The findings displayed in Table 1 unmistakably demonstrated that the inclusion of CNC particles led to an elevation in the opacity value of the obtained bionanocomposite films.[60] The data indicates that the CS/PVA bionanocomposite film exhibited the lowest opacity (0.6882) and, consequently, the highest level of transparency. The introduction of CNC had a significant impact on elevating the film's opacity, primarily attributed to the increased reinforcement value and interaction of CNC with CS/PVA, as evident from the tensile data. The addition of CNCs to the CS/PVA film results in opacity values of 0.6882 for CS/PVA, 0.7441 for CS/PVA/CNC-0.5%, 0.7457 for CS/PVA/CNC-1%, 1.0773 for CS/PVA/CNC-2.5%, and 1.3950 for CS/PVA/CNC-5%. This could be attributed to the obstruction of the light pathway within the well-formed matrix, resulting from the robust

Table 1 Thickness and opacity values of the bionanocomposite films

Sample	Thickness (mm)	Opacity$_{600}$
CS/PVA	0.06	0.6882
CS/PVA/CNC-0.5%	0.06	0.7441
CS/PVA/CNC-1%	0.06	0.7457
CS/PVA/CNC-2.5%	0.06	1.0773
CS/PVA/CNC-5%	0.06	1.3950

interaction among CS, PVA, and CNC. Opacity is observed to be directly linked to the even distribution of film components and is contingent upon the film's internal structure. Furthermore, the reduction in transparency was also a consequence of enhanced light scattering caused by the cellulose nanocrystals. As such, the bionanocomposite films can be classified as having a level of transparency. Generally, films with reduced UV and visible light transmission, characterized by their opacity, serve as suitable packaging materials for minimizing food oxidative degradation, which can result in color changes, nutrient degradation, and undesirable flavors.[61]

Water solubility

Hydrophilic substances take in water molecules through immediate contact with water or from their surrounding environment. One of the main drawbacks of the CS, PVA, and CNC is that they are highly hydrophilic compounds. However, this drawback is critically important for promoting environmentally sustainable material deterioration. The abundance of hydroxyl groups makes them hydrophilic as they are strongly polar and react quickly to the presence of water.[62,63] The water absorption of polymer films is a crucial factor in determining their durability. The water solubility results of the unreinforced CS/PVA film and CS/PVA film reinforced with 0.5–1 and 2.5 wt% CNC were evaluated and illustrated in Fig. 12. The film composed entirely of CS and PVA showed the highest level of film solubility, measuring in at 48%. When the amount of CNC in the film went from 0.5 wt%, 1 wt% then to 2.5 wt%, the film's solubility decreased significantly, falling from 47% to 43% and then from 43% to 33% accordingly. Consequently, the inclusion of CNC into the blend reduced its water absorption due to the construction of a compact three-dimensional structure involving the polymeric matrix and the molecules of CNC through hydrogen bonding. This effect limits the chain's freedom of movement, lessens the number of free hydroxyl groups in the matrix, and prevents water from penetrating the molecular structure. Since the water molecules were unable to break down the hydrogen bonds, the film's solubility decreased.[64]
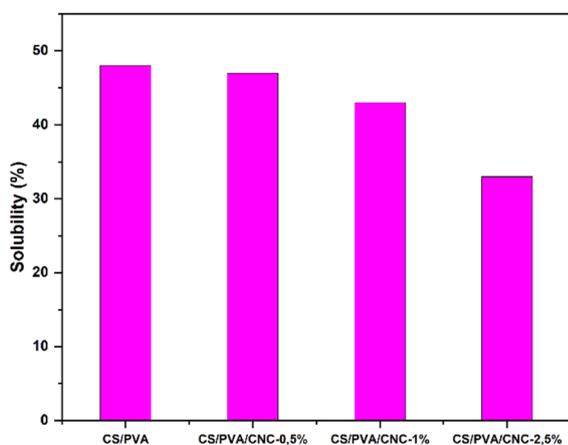
Fig. 12   Water solubility of the bio-nanocomposites films.

Conclusion

Throughout the course of this research, non-polluting bio-nanocomposites films based on polyvinyl alcohol (PVA) and chitosan (CS) blend strengthened with cellulose nanocrystals (CNCs) have been developed. Through a sulfuric acid hydrolysis approach, the CNC nano-reinforcing agent were separated at the nanometric scale from hemp stalks. The effective removal of non-cellulosic chemicals was indicated by the FTIR, OM and SEM examination. The obtained CNC had a small size including a diameter of 6.38 ± 1.27 nm and a length equal to 277.76 ± 61 nm. This latter was then successfully distributed in a CS/PVA blend to form CS/PVA/CNC (0, 0.5, 1, 2.5 and 5%) bionano-composite films *via* solvent casting method. The data obtained from FTIR revealed the presence of robust hydrogen bonding connections between PVA and CS chains, as well as between the CS/PVA blend and CNCs. The SEM pictures show that the CS/PVA/CNC bionanocomposite films formed smoothly, without any clumping or aggregation. Because of the relatively elevated aspect ratio of CNCs derived from hemp fibers (44.69 ± 11.08), their inclusion in CS/PVA blend had a beneficial impact on the characteristics of the resulting bionanocomposite films. Incorporating CNCs into the CS/PVA film, up to a weight percentage of 5%, led to enhancement in both Young's modulus and tensile strength of the bionanocomposite films, measuring at (412.46 ± 10.49 MPa) and (18.60 ± 3.42 MPa), respectively. This marked an improvement compared to the CS/PVA film, which exhibited values of (202.32 ± 22.50 MPa) and (13.72 ± 2.61 MPa), respectively. Furthermore, the bionanocomposite films preserved almost the level of transparency as the CS/PVA blend material, indicating the good distribution of CNC on a nano-metric level. However, the incorporation of CNCs up to 5% into the bionanocomposite films resulted in a decrease in the gas transmission rate (from 7.013 to 4.159 cm³ (m² day·0.1 MPa))⁻¹ and water solubility (from 48% to 33%). All can be attributed to the establishment of a complex network structure which creates a convoluted pathway inside the composite film. This research aimed to enhance the value of Moroccan hemp stalks by utilizing them in the extraction of nanoscale cellulose crystals and assessing their potential for strengthening biopolymer mixture to generate the previously mentioned bionanocomposite films characterized by favourable chemical and mechanical attributes. Based on the findings and in terms of perspectives, we are willing to consider conducting comparative studies with other sources of natural fibers, focus on optimizing the production processes to enhance the properties of the biona-nocomposite films and conducting their antimicrobial and antioxidant activities. By addressing these perspectives, it is expected that these eco-friendly, highly functional, and structurally advanced bionanocomposite films will find promising applications in the food packaging area.

Author contributions

Kenza Bahsaine: data curation; investigation; visualization; methodology; writing – original draft. Brahim El Allaoui: data curation; investigation; visualization; methodology; writing –

original draft. Hanane Benzeid: supervision, writing – review & editing. Nadia Zari: writing – original draft; writing – review & editing. Abou el kacem Qaiss: conceptualization; supervision; review & editing, Rachid Bouhfid: conceptualization; supervision; review & editing.

Conflicts of interest

There are no conflicts to declare.

Acknowledgements

Notes and references

1 B. P. Anand, B. N. Reshma, P. S. Sellamuthu, E. R. Sadiku, X. Li and Y. He, *Chemosphere*, 2022, **287**(2), 132084, DOI: **10.1016/j.chemosphere.2021.132084**.

2 H. Yousefi, H. M. Su, S. M. Imani, K. Alkhaldi, C. D. Filipe and T. F. Didar, *ACS Sens.*, 2019, **4**(4), 808–821, DOI: **10.1021/acssensors.9b00440**.

3 A. A. Oun, G. H. Shin, J.-W. Rhim and J. T. Kim, *Food Packag. Shelf Life*, 2022, **34**, 100991, DOI: **10.1016/j.fpsl.2022.100991**.

4 H. C. Oyeoka, C. M. Ewulonu, I. C. Nwuzor, C. M. Obele and J. T. Nwabanne, *J. Bioresour. Bioprod.*, 2021, **6**(2), 168–185, DOI: **10.1016/j.jobab.2021.02.009**.

5 J. N. N. Bueno, E. Corradini, P. R. de Souza, V. de S. Marques, E. Radovanovic and E. C. Muniz, *Polym. Test.*, 2021, **101**, 107279, DOI: **10.1016/j.polymertesting.2021.107279**.

6 Annu, A. Ali and S. Ahmed, *Heliyon*, 2021, 7(3), e06550, DOI: **10.1016/j.heliyon.2021.e06550**.

7 J. P. S. Morais, M. d. F. Rosa, M. d. s. M. d. S. Filho, L. D. Nascimento, D. M. do Nascimento and A. R. Cassâtes, *Carbohydr. Polym.*, 2013, **91**, 229–235, DOI: **10.1016/j.carbpol.2012.08.010**.

8 R. Vijay, D. Lenin Singaravelu, A. Vinod, M. R. Sanjay, S. Siengchin, M. Jawaid, A. Khan and J. Parameswaranpillai, *Int. J. Biol. Macromol.*, 2019, **125**, 99–108, DOI: **10.1016/j.ijbiomac.2018.12.056**.

9 K. Bahsaine, H. Chakhtouna, M. E. M. Mekhzoum, N. Zari, H. Benzeid, A. Qaiss and R. Bouhfid, *Biomass Convers. Biorefin.*, 2023, DOI: **10.1007/s13399-023-04130-y**.

10 N. Reddy and Y. Yang, *Trends Biotechnol.*, 2005, **23**(1), 22–27, DOI: **10.1016/j.tibtech.2004.11.002**.

11 V. Bansal, P. Sharma, N. Sharma, P. Pal and R. Malviya, *Adv. Biol. Res.*, 2011, **5**, 28–37.

12 T. Huber, J. Müssig, O. Curnow, S. Pang, S. Bickerton and M. S. Staiger, *J. Mater. Sci.*, 2012, 1171–1186, DOI: **10.1007/s10853-011-5774-3**.

13 A. J. Morán, V. A. Alvarez, V. P. Cyras and A. Vázquez, *Cellulose*, 2008, **15**, 149–159, DOI: **10.1007/s10570-007-9145-9**.

14 A. H. Tayeb, E. Amini, S. Ghasemi and M. Tajvidi, *Molecules*, 2018, **23**, 1–24, DOI: **10.3390/molecules23102684**.

15 T. Heinze, Cellulose: Structure and Properties, in *Cellulose Chemistry and Properties: Fibers, Nanocelluloses and*

Advanced Materials, Advances in Polymer Science, ed. O. Rojas, Springer, Cham, 2015, vol. 271, DOI: **10.1007/12_2015_319**.

16 H. Du, W. Liu, M. Zhang, C. Si, X. Zhang and B. Li, *Carbohydr. Polym.*, 2019, **209**, 130–144, DOI: **10.1016/j.carbpol.2019.01.020**.

17 T. Townsend, World Natural Fibre Production and Employment, in *Handbook of Natural Fibres*, Woodhead Publishing Series in Textiles, ed. R. M. Kozłowski and M. Mackiewicz-Talarczyk, Woodhead Publishing, 2nd edn, 2020, pp. 15–36.

18 M. M. Kabir, H. Wang, K. T. Lau and F. Cardona, *Composites, Part B*, 2013, **53**, 362–368, DOI: **10.1016/j.compositesb.2013.05.048**.

19 H. N. Dhakal and Z. Zhang, *Biofiber Reinf. Compos. Mater.*, 2015, 86–103, DOI: **10.1533/9781782421276.1.86**.

20 S. Dixit, G. Mishra and V. L. Yadav, *Polym. Bull.*, 2022, **79**, 2559–2583, DOI: **10.1007/s00289-021-03646-5**.

21 M. Flórez, E. Guerra-Rodríguez, P. Cazón and M. Vázquez, *Food Hydrocolloids*, 2022, **124**, 107328, DOI: **10.1016/j.foodhyd.2021.107328**.

22 D. Debomitra, V. Dharini, S. Periyar Selvam, R. E. Sadiku, M. Mahesh Kumar, J. Jayaramudu and U. N. Gupta, *Mater. Today: Proc.*, 2021, **38**, 860–869, DOI: **10.1016/j.matpr.2020.04.885**.

23 M. Raji, A. Halloub, A. Qaiss and R. Bouhfid, in *Handbook of Bioplastics and Biocomposites Engineering Applications*, ed. T. A. Inamuddin, Wiley, 2nd edn, 2023, pp. 457–470.

24 A. M. Abdelghany, A. A. Menazea and A. M. Ismail, *J. Mol. Struct.*, 2019, **1197**, 603–609, DOI: **10.1016/j.molstruc.2019.07.089**.

25 J. R. A. Pires, V. G. L. de Souza and A. L. Fernando, *Food Packag. Shelf Life*, 2018, **17**, 142–149, DOI: **10.1016/j.fpsl.2018.06.011**.

26 M. Kostag and O. A. El Seoud, *Carbohydr. Polym. Technol. Appl.*, 2021, **2**, 100079, DOI: **10.1016/j.carpta.2021.100079**.

27 A. Sionkowska, *Prog. Polym. Sci.*, 2011, **36**(9), 1254–1276, DOI: **10.1016/j.progpolymsci.2011.05.003**.

28 K. El Bourakadi, N. Merghoub, M. Fardioui, M. E. M. Mekhzoum, I. M. Kadmiri, E. M. Essassi, A. E. K. Qaiss and R. Bouhfid, *Composites, Part B*, 2019, **172**(1), 103–110, DOI: **10.1016/j.compositesb.2019.05.042**.

29 P. S. Sellamuthu, R. B. Nambiar and E. R. Sadiku, *Appl. Surf. Sci.*, 2018, **449**, 591–602, DOI: **10.1016/j.apsusc.2018.01.022**.

30 A. B. Perumal, R. B. Nambiar, P. S. Sellamuthu, E. R. Sadiku, X. Li and Y. He, *Chemosphere*, 2022, **287**, 132084, DOI: **10.1016/j.chemosphere.2021.132084**.

31 M. Fardioui, A. Stambouli, T. Gueddira, A. Qaiss and R. Bouhfid, *J. Polym. Environ.*, 2016, **24**, 356–362, DOI: **10.1007/s10924-016-0784-5**.

32 A. Halloub, M. Raji, H. Essabir, S. Nekhlaoui, M.-O. Bensalah, R. Bouhfid and A. Qaiss, *Int. J. Biol. Macromol.*, 2023, **234**, 123764, DOI: **10.1016/j.ijbiomac.2023.123764**.

33 Z. Belouadah, A. Ati and M. Rokbi, *Carbohydr. Polym.*, 2015, **134**, 429–437, DOI: **10.1016/j.carbpol.2015.08.024**.

34 M. Maache, A. Bezazi, S. Amroune, F. Scarpa and A. Dufresne, *Carbohydr. Polym.*, 2017, **171**, 163–172, DOI: 10.1016/j.carbpol.2017.04.096.

35 A. Dghoughi, F.-E. Nazih, A. Halloub, M. Raji, H. Essabir, M. Ouadi Bensalah, R. Bouhfid and A. Qaiss, *Int. J. Biol. Macromol.*, 2023, **242**, 125077, DOI: 10.1016/j.ijbiomac.2023.125077.

36 K. O. Reddy, B. Ashok, K. R. N. Reddy and Y. E. Feng, *Int. J. Polym. Anal. Charact.*, 2014, **19**, 48–61, DOI: 10.1080/1023666X.2014.854520.

37 S. S. Saravanakumar, A. Kumaravel, T. Nagarajan, P. Sudhakar and R. Baskaran, *Carbohydr. Polym.*, 2013, **92**, 1928–1933, DOI: 10.1016/j.carbpol.2012.11.064.

38 T. P. Sathishkumar, P. Navaneethakrishnan, S. Shankar, R. Rajasekar and N. Rajini, *J. Reinf. Plast. Compos.*, 2013, **32**(19), 1457–1476, DOI: 10.1177/0731684413495322.

39 Z. Kassab, Y. Abdellaoui, M. H. Salim, R. Bouhfid, A. Qaiss and M. El Achaby, *Carbohydr. Polym.*, 2020, **245**, 116506, DOI: 10.1016/j.carbpol.2020.116506.

40 A. Bahloul, Z. Kassab, M. El Bouchti, H. Hannache, A. El, K. Qaiss, M. Oumam and M. El Achaby, *Carbohydr. Polym.*, 2021, **253**, 117311, DOI: 10.1016/j.carbpol.2020.117311.

41 Y. Zhao, C. Moser, M. E. Lindström, G. Henriksson and J. Li, *ACS Appl. Mater. Interfaces*, 2017, **9**(15), 13508–13519, DOI: 10.1021/acsami.7b01738.

42 V. Mikulcova, R. Bordes, A. Minarik and V. Kasparkova, *Food Hydrocolloids*, 2018, **80**, 60–67, DOI: 10.1016/j.foodhyd.2018.01.034.

43 M. G. A. Efendy and K. L. Pickering, *Composites, Part A*, 2014, **67**, 259–267, DOI: 10.1016/j.compositesa.2014.08.023.

44 A. Sair, S. Oushabi, A. Kammouni, A. Tanane, O. Abboud, Y. Oudrhiri Hassani, F. Laachachi and A. El Bouari, *Case Stud. Therm. Eng.*, 2017, **10**, 550–559, DOI: 10.1016/j.csite.2017.10.012.

45 T. Väisänen, P. Batello, R. Lappalainen and L. Tomppo, *Ind. Crops Prod.*, 2018, **111**, 422–429, DOI: 10.1016/j.indcrop.2017.10.049.

46 S. J. Eichhorn, A. Dufresne, M. Aranguren, N. E. Marcovich, J. R. Capadona, S. J. Rowan, C. Weder, W. Thielemans, M. Roman, S. Renneckar, W. Gindl, S. Veigel, J. Keckes, H. Yano, K. Abe, M. Nogi, A. N. Nakagaito, A. Mangalam, J. Simonsen, A. S. Benight, A. Bismarck, L. A. Berglund and T. Peijs, *J. Mater. Sci.*, 2010, **45**, 1–33, DOI: 10.1007/s10853-009-3874-0.

47 N. M. Mahmoodi, M. Oveisi, A. Taghizadeh and M. Taghizadeh, *Carbohydr. Polym.*, 2019, **227**, 115364, DOI: 10.1016/j.carbpol.2019.115364.

48 G. Yuvaraja, J. L. Pathak, Z. Weijiang, Z. Yaping and X. Jiao, *Int. J. Biol. Macromol.*, 2017, **103**, 234–241, DOI: 10.1016/j.ijbiomac.2017.05.020.

49 J. Bonilla, E. Fortunati, L. Atarés, A. Chiralt and J. M. Kenny, *Food Hydrocolloids*, 2014, **35**, 463–470, DOI: 10.1016/j.foodhyd.2013.07.002.

50 E. Fortunati, P. Benincasa, G. M. Balestra, F. Luzi, A. Mazzaglia, D. Del Buono, D. Puglia and L. Torre, *Ind. Crops Prod.*, 2016, **92**, 201–217, DOI: 10.1016/j.indcrop.2016.07.047.

51 H. Yu, B. Sun, D. Zhang, G. Chen, X. Yang and J. Yao, *J. Mater. Chem. B*, 2014, **48**(2), 8479–8489, DOI: 10.1039/C4TB01372G.

52 B. M. Trinh, B. P. Chang and T. H. Mekonnen, *Prog. Mater. Sci.*, 2023, **133**, 101071, DOI: 10.1016/j.pmatsci.2023.101071.

53 S. Van Nguyen and B. K. Lee, *Carbohydr. Polym.*, 2022, **298**, 120064, DOI: 10.1016/j.carbpol.2022.120064.

54 W. Hong, B. Ghanbarzadeh, H. Fasihi and R. Montazami, *Int. J. Biol. Macromol.*, 2018, **107**, 2065–2074, DOI: 10.1016/j.ijbiomac.2017.10.083.

55 S. Xu, M. Jiang, Q. Lu, S. Gao, J. Feng, X. Wang, X. He, K. Chen, Y. Li and P. Ouyang, *Front. Bioeng. Biotechnol.*, 2020, **8**, 1–11.

56 L. Li, W. Wang, J. Sun, Z. Chen, Q. Ma, H. Ke and J. Yang, *Food Packag. Shelf Life*, 2022, **34**, 100985, DOI: 10.1016/j.fpsl.2022.100985.

57 S. Azizi, M. Bin Ahmad, N. A. Ibrahim, M. Z. Hussein and F. Namvar, *Chin. J. Polym. Sci.*, 2014, **32**, 1620–1627, DOI: 10.1007/s10118-014-1548-0.

58 M. Boo, Y. Wang, I. Zucker, Y. Choo, C. O. Osuji and M. Elimelech, *Environ. Sci. Technol.*, 2018, **52**(13), 7279–7288, DOI: 10.1021/acs.est.8b01040.

59 M. Yadav, K. Behera, Y.-H. Chang and F.-C. Chiu, *Polymers*, 2020, **12**, 202, DOI: 10.3390/polym12010202.

60 L. Motelica, D. Ficai, O. Oprea, A. Ficai, R.-D. Trusca, E. Andronescu and A. M. Holban, *Pharmaceutics*, 2021, **13**, 1020, DOI: 10.3390/pharmaceutics13071020.

61 M. Salari, M. S. Khiabani, R. R. Mokarram, B. Ghanbarzadeh and H. S. Kafil, *Food Hydrocolloids*, 2018, **84**, 414–423, DOI: 10.1016/j.foodhyd.2018.05.037.

62 H. C. Oyeoka, C. M. Ewulonu, I. C. Nwuzor, C. M. Obele and J. T. Nwabanne, *J. Bioresour. Bioprod.*, 2021, **6**(2), 168–185, DOI: 10.1016/j.jobab.2021.02.009.

63 F. Ahmadi, Z. Oveisi, M. Samani and Z. Amoozgar, *Res. Pharm. Sci.*, 2015, **10**, 1–16.

64 P. G. Gan, S. T. Sam, M. F. Abdullah and M. Firdaus Omar, *Polym. Degrad. Stab.*, 2021, **188**, 109563, DOI: 10.1016/j.polymdegradstab.2021.109563.